

MAGNETIC CIRCUIT DESIGN OF A BEARINGLESS SINGLE-PHASE SLICE MOTOR

**Klaus Nenninger, Wolfgang Amrhein, Siegfried Silber,
Gernot Trauner, Martin Reisinger**
LCM - Linz Center of Competence in Mechatronics
Johannes Kepler University of Linz
A-4040 Linz, Austria
nenninger@mechatronik.uni-linz.ac.at

ABSTRACT

For plenty of applications a very simple mechanical design of a bearingless motor can be employed. With the so-called slice motor the complexity of a bearingless motor can potentially be reduced. As a result of the disk rotor design only three spatial degrees of freedom have to be controlled actively, the x- and y-positions of the rotor plane and the rotary angle. The axial position and the tilt angle are stabilized passively by the magnetic reluctance forces. In this paper the influence of the magnetic circuit design on the passive stability is investigated. At first the geometry of the permanent magnet rotor is optimized with the help of three dimension finite element analysis of the magnetic circuit. Afterwards the results from these finite element calculations are evaluated by means of the mechanical model of the rotor disk which also considers the gyro dynamics of the rotating disk.

INTRODUCTION

Bearingless motors offer various possibilities in special applications with high demands on cleanliness (no lubrication), tightness (no seal) or lifetime (no wear) where conventional bearing can hardly persist [1] - [3]. Additionally, it is practicable to influence the performance of the drive and therefore the operating behavior of the whole application by engaging the control loop of the active magnetic bearing. A commonly used method is for example active vibration control [4], [5]. An other approach to use the extensive system of active magnetic bearing as an advantage is to determine process values like flow or pressure in a pump from already measured bearing parameters without the necessity of additional sensors [6]. However, especially for low-cost applications the complexity in mechanical and electrical design must be

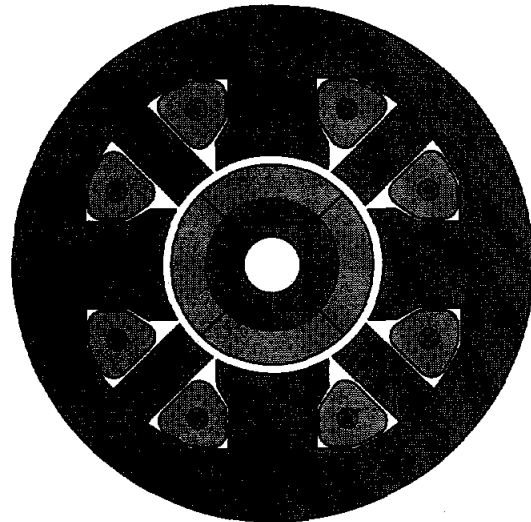


FIGURE 1: Bearingless single-phase motor with four concentrated fractional pitch coils for radial force and torque generation

kept as small as possible to reduce costs. For several arrangements where external process forces are within a moderate range a very simple construction in the form of a slice motor design can be employed [7] - [10].

The bearingless motor in Figure 1 is a four-pole single-phase motor with concentrated fractional pitch windings.

For optimal levitation force control the permanent magnet excitation of the slice rotor should generate a sinusoidal flux density distribution in the air gap. To achieve full operation two orthogonal two pole armature fields for levitation control and a four pole armature

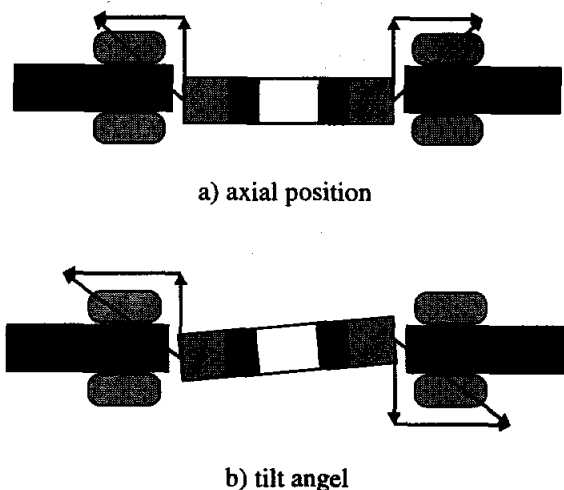


FIGURE 2: Passive stabilization of axial position and tilt angles of the slice rotor

field for rotation control are required. For the discussed motor only one winding system with four concentrated coils is used to control both radial force (two pole fields) and torque (four pole field). This is realized by superposition of the current components responsible for levitation force and torque in the control algorithm. The shape of the stator stack in Figure 1 with the intermediate poles has already been optimized with respect to active control of levitation force [11].

As a result of the disk rotor design only three spatial degrees of freedom have to be controlled actively. These are the x - and y -directions of the rotor plane and the rotary angle. The axial position and the tilt angles are stabilized passively by the magnetic tensile force and an appropriate selected diameter / axial-length ratio of the permanent magnet rotor. Figure 2 a shows the stabilization of the axial position. Figure 2 b explains the stabilization of the tilt angle.

The above mentioned technique of passive stabilization of three spatial degrees of freedom is investigated in more detail in the following paragraphs.

First of all the magnetic circuit design is analyzed concerning the influence of different parameters on the stiffness of the passive stabilized axes. The appropriate calculations are executed by means of a three dimension finite element program.

Further steps are to evaluate the results from the finite element calculations and their effects on the mechanical stability in terms of gyroscopic effects acting on the rotating disk.

MAGNETIC CIRCUIT DESIGN

Various geometric parameters, material properties and their combinations are analyzed to find the magnetic

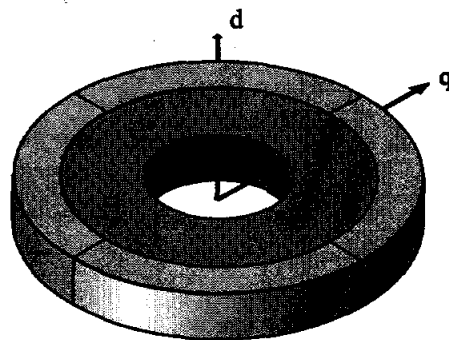


FIGURE 3: Definition of the d - and q -directions of the four pole slice rotor with sinusoidal flux density distribution in the air gap

circuit design for maximum stiffness of the passive stabilized axes of the slice rotor.

To keep the number of possible combinations within an acceptable amount it is assumed that one of the geometric dimensions is predetermined by the application. This predetermined geometric value should be the diameter of the rotor.

Consequently, all geometric parameters relate to this diameter and therefore the amount of variations is limited. Additionally, the air gap length is fixed by the application. The other dimensions of the stator details do not influence the calculation results as long as saturation is prevented. Therefore the stator details are not taken into account anymore in the further paragraphs.

Definition of the Tilting Directions

As mentioned before the four pole permanent magnet rotor generates a sinusoidal flux density distribution in the air gap. According to this distribution two main directions can be defined. The d -direction which points toward the maximum of the flux density and the q -direction which marks the zero value of the flux density distribution (see Figure 3).

Passive Stiffness

When the rotor is tilted according to Figure 2 b without any axial displacement, the passive turn back moment of the tilted rotor disk is shown in Figure 4. It is substantial that there is practically no difference in the passive turn back moment between tilting vertical to d -direction or tilting vertical to q -direction. Therefore, the static tilting stiffness which is represented by this turn back moment can be handled as independent from the tilting direction. This is only valid for a four pole rotor. A two pole rotor shows a significant discrepancy in the

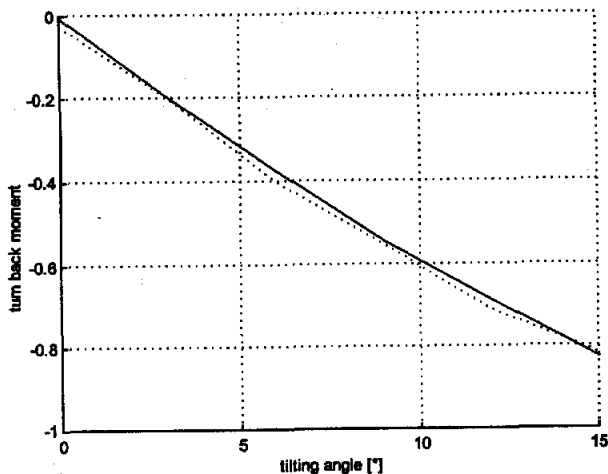


FIGURE 4: Passive turn back moment of the tilted rotor disk for different tilting directions and a certain axial length of the rotor (solid line: vertical to d-direction, dotted line: vertical to q-direction)

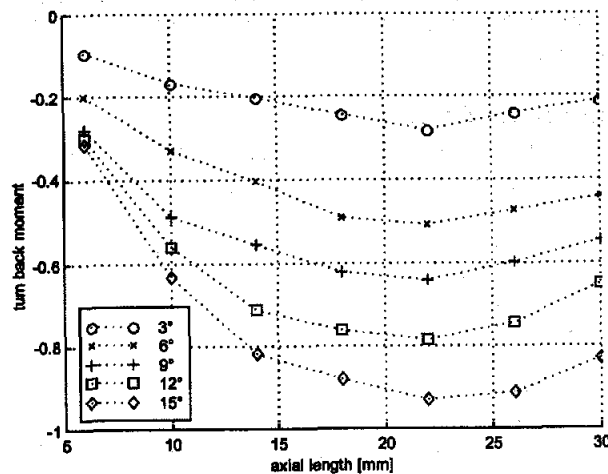


FIGURE 5: Passive turn back moment of the tilted rotor disk for different axial length and different tilting angles

passive turn back moment between d- and q-direction which can not be neglected.

Another interesting fact which can be seen from Figure 4 is that the passive static stiffness can be considered as constant around the origin within tilting angles of $\pm 9^\circ$.

Subsequently, the diameter / axial-length ratio of the permanent magnet rotor is analyzed. It should be investigated what ratio is the optimum concerning the static tilting stiffness. Figure 5 shows that the turn back moment increases with the axial length of the rotor when the diameter is kept constant. After reaching a maximum at a certain ratio it decreases again.

Results from the Finite Element Calculation

From the diagram in Figure 5 the optimal axial length is about 22 mm for the predetermined diameter. Furthermore, for the investigated constellation, it can clearly be seen, that the tilting stiffness is constant within a tilting angle of about $\pm 9^\circ$ and independent from the tilting direction.

Additional Calculations and Considerations

In addition to the discussed results a various number of simulations are done. For example the whole motor is split apart in the xy-plane and the two parts are moved apart along the z-axis. The gap between the two parts is filled with air or non-ferromagnetic material. That is the axial length of the motor is increased without adding extra iron or permanent magnet material. The results

show that the passive stiffness decreases under this circumstances. That means not only the leakage flux at the fronts end is crucial for the passive stabilization but also the structure of the whole air gap influences the stiffness.

In the same way the selection of material affects the passive stiffness. As expected, the higher the magnetic energy density of the permanent magnets the higher the passive stiffness of the rotor disk for unchanged geometry.

An other interesting fact is that the passive stiffness in tilting direction depends on movements in z-direction. Therefore, the following considerations are for a static operating point (that is static z-displacement) which can also be influenced by the design of the application.

Other simulations show that the optimal diameter / axial-length ratio from Figure 5 is also very useful for the stabilization of the axial displacement in z-direction within the expected ranges.

MECHANICAL BEHAVIOR OF THE ROTOR

In the following the results from the finite element calculation and their effects on the dynamic behavior of the rotor in terms of gyroscopic effects acting on the rotating disk are evaluated [12], [13]. For these considerations the mechanical model of the levitated rotor disk is set up.

Damping in the actively stabilized directions can be influenced by control and should not be part in the following modeling. Damping of the passively stabilized movements depend on the application and

need to be identified for each constellation. Thus only natural vibrations without damping are taken into account.

Equation of Motion

The model of the rotor (see Figure 6) should have the following properties:

- The rotor is a rigid circular disk with mass m and polar and diametric moments of inertia I_p and I_d respectively.
- No unbalance force and moment exist.
- The center of mass S is coincident with the center of rotation.
- The drive part of the bearingless motor is giving a constant rotational speed Ω . Furthermore, the whole application is running at a static operating point with static z -displacement.
- The actively controlled levitation forces are acting on the mass center S of the rotating disk.

The displacements in x - and y -directions and the angular movements α and β of the disk are determined by Figure 6. F_x , F_y , M_α and M_β are the corresponding forces and moments.

The equations of motion can be written as

$$\begin{aligned} m\ddot{x} &= \sum F_x \\ m\ddot{y} &= \sum F_y \\ \dot{D}_\alpha &= \sum M_\alpha \\ \dot{D}_\beta &= \sum M_\beta \end{aligned} \quad (1)$$

The forces F_x and F_y are functions of displacement and current linearized about the operating point [10] and are described by the commonly used expressions

$$\begin{aligned} F_x &= k_s x + k_i i_x \\ F_y &= k_s y + k_i i_y \end{aligned} \quad (2)$$

where k_s is the force-displacement factor and k_i the current-force factor of the active magnetic bearing [12]. It is assumed that the bearing shows the same behavior in both x - and y -directions.

The time derivatives of the angular moments D_α and D_β are determined by the linearized equations of gyroscopic movement [14]

$$\begin{aligned} \dot{D}_\alpha &= I_d \ddot{\alpha} + I_p \Omega \dot{\beta} \\ \dot{D}_\beta &= I_d \ddot{\beta} - I_p \Omega \dot{\alpha} \end{aligned} \quad (3)$$

The related moments M_α and M_β are defined by the tilting stiffness k_t

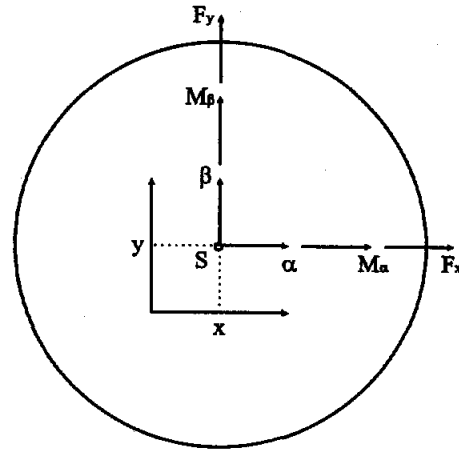


FIGURE 6: Model of the rotating disk

$$\begin{aligned} M_\alpha &= k_t \alpha \\ M_\beta &= k_t \beta \end{aligned} \quad (4)$$

obtained from the finite element calculations. As discussed above, the disk shows the same stiffness in α - and β -tilting directions.

Equations (1) - (4) can be combined to

$$\mathbf{M}\ddot{\mathbf{x}} + \mathbf{G}\dot{\mathbf{x}} + \mathbf{K}_s \mathbf{x} + \mathbf{K}_i \mathbf{i} = \mathbf{0} \quad (5)$$

with the mass matrix

$$\mathbf{M} = \begin{bmatrix} m & 0 & 0 & 0 \\ 0 & m & 0 & 0 \\ 0 & 0 & I_d & 0 \\ 0 & 0 & 0 & I_d \end{bmatrix},$$

the gyroscopic matrix

$$\mathbf{G} = \begin{bmatrix} 0 & 0 & 0 & 0 \\ 0 & 0 & 0 & 0 \\ 0 & 0 & 0 & I_p \Omega \\ 0 & 0 & -I_p \Omega & 0 \end{bmatrix},$$

and the stiffness matrices

$$\mathbf{K}_s = \begin{bmatrix} k_s & 0 & 0 & 0 \\ 0 & k_s & 0 & 0 \\ 0 & 0 & k_t & 0 \\ 0 & 0 & 0 & k_t \end{bmatrix} \quad \text{and} \quad \mathbf{K}_i = \begin{bmatrix} k_i & 0 & 0 & 0 \\ 0 & k_i & 0 & 0 \\ 0 & 0 & 0 & 0 \\ 0 & 0 & 0 & 0 \end{bmatrix},$$

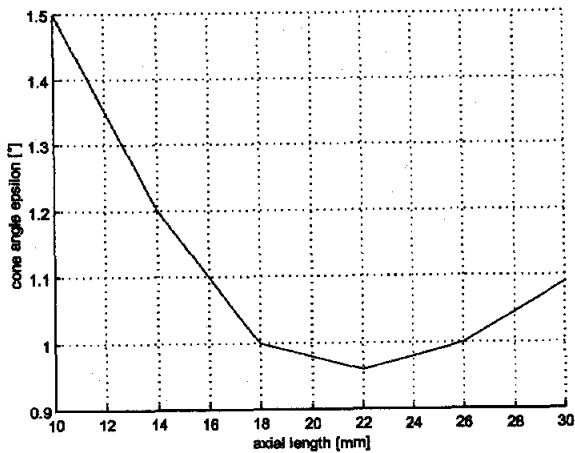


FIGURE 7: Influence of the axial length on the cone angle ϵ of the nutation initiated by a moment step in tilting direction

furthermore, the displacement vector

$$\mathbf{x} = [x \ y \ \alpha \ \beta]^T$$

and the control input vector

$$\mathbf{i} = [i_x \ i_y \ 0 \ 0]^T$$

Discussion

From Equation (5) can be seen that the tilting movements are decoupled from the plane motion of the mass center, assuming that the passive tilting stiffness is not influenced by the levitation current.

Therefore, in the following considerations of the passive stability only the tilting movements are taken into account.

The cone angle ϵ of the nutation initiated by a moment step in tilting direction is evaluated by simulation. The results are shown in Figure 7 for a rotating speed of 10000 rpm.

For the actual configuration the increasing stiffness caused by the spin of the rotor [12] appears only on much higher rotational speeds than in the provided applications are useful. For rotating speeds of about 10000 rpm the stiffness caused by the magnetic tensile force is dominant. Furthermore, for the investigated diameter/axial length ratios the stabilizing effect of thin shaped disks with respect to different moments of inertia is covered by the magnetic turn back force, as well.



FIGURE 7: Bearingless single-phase slice motor with concentrated fractional pitch coils

Thus, suitable to the previous results from the finite element calculation the optimal axial length is again about 22 mm for the predetermined diameter of the rotor.

SUMMARY AND OUTLOOK

Figure 8 shows the prototype of the bearingless single-phase slice motor. Some experimental tests concerning the passive stability of the rotor disk have been performed on this prototype. The axial length of the prototype is only 14 mm. Therefore, it does not have the optimal diameter/axial length ratio, nevertheless, the measured or identified values fit very well to the simulated results.

Verified values are the passive tilting stiffness which are conform to the simulated one in magnitude and independence of direction.

Furthermore, the frequency of the measured vibrations of the passive stabilized rotor fit together with the results from Equation (5).

Thus, the simplified model of the levitated slice rotor seems to be accurate enough for the analyses of the passive stability.

In future steps two additional motors are manufactured one with an extra thin (short) rotor and one with optimal diameter/axial length ratio to verify and improve the model for these extreme cases.

ACKNOWLEDGMENTS

The project is partly kindly supported by Levitronix GmbH Zurich, the Austrian and Upper Austrian government and the Johannes Kepler University of Linz. The authors thank all involved partners for their support.

REFERENCES

1. Schöb R., Dasse K., Magnetic Suspension Systems for Biomedical Applications, Proc. 6th Int. Symp. on Magnetic Suspension Technology, Turin Italy 2001
2. Neff M., Barletta N., Schöb R., Bearingless Pump System for Semiconductor Industrie, Proc. 6th Int. Symp. on Magnetic Suspension Technology, Turin Italy 2001
3. Ueno S., Chen C. Ohishi T., Matsuda K., Okada Y. Taenaka Y., Masuzawa T., Design of a Self-Bearing Slice Motor for a Centrifugal Blood Pump, Proc. of the Power Conversion Intelligent Motion, Nürnberg Germany 1998
4. Takemoto M, Chiba A., Fukao T., A Feed-Forward Comp. For Vibration Reduction Considering Magn. Attraction Force in Bearingless SR-Motors, Proc. 7th Int. Symp. on Magnetic Bearings, Zurich Switzerland 2000
5. Hüttner Ch., Schöb R., Vibration Control for a Bearingless Slice Motor of an Implantable Blood Pump, Proc. 6th Int. Symp. on Magnetic Suspension Technology, Turin Italy 2001
6. Hahn J., Schöb R., Determining Flow and Pressure in a Bearingless Pump from Radial Magnetic Forces, Proc. 6th Int. Symp. on Magnetic Suspension Technology, Turin Italy 2001
7. Barletta N., Der lagerlose Scheibenmotor, Dissertation, ETH Zürich 1998
8. Schöb R., Barletta N., Principle and Application of a Bearingless Slice Motor, Proc. 5th Int. Symp. on Magnetic Bearings, Kanazawa Japan 1996
9. Amrhein W., Silber S., Bearingless single-phase brushless DC motor, Proc. of the Symp. on Power Electronics Electrical Drives Advanced Machines Power Quality '98, Sorrento Italy 1998
10. Silber S., Beiträge zum lagerlosen Einphasenmotor, Dissertation, Johannes Kepler Universität Linz 2000
11. Nenninger K., Amrhein W., Silber S., Bearingless Single-Phase Motor with Fractional Pitch Windings, Proc. 7th Int. Symp. on Magnetic Bearings, Zurich Switzerland 2000
12. Schweitzer G., Bleuler H., Traxler A., Active Magnetic Bearings, vdf-Hochschulverlag 1994
13. Krämer E., Dynamics of Rotors and Foundations, Springer-Verlag 1993
14. Czichos H., Hütte, Die Grundlagen der Ingenieurwissenschaften, Springer-Verlag 1996